Resonant Raman scattering due to bound-carrier spin flip in $GaAs/Al_xGa_{1-x}As$ quantum wells

V.F. Sapega,* T. Ruf, M. Cardona, and K. Ploog
Max-Planck-Institut für Festkörperforschung, Heisenbergstrasse 1, D-70569 Stuttgart, Federal Republic of Germany

E.L. Ivchenko and D.N. Mirlin
A.F. Ioffe Physico-Technical Institute, Russian Academy of Sciences, 194021 St. Petersburg, Russia
(Received 18 March 1994)

We study Raman scattering by spin flips of acceptor-bound holes in p-type $GaAs/Al_xGa_{1-x}As$ multiple quantum wells in normal and tilted magnetic fields. It is shown that different mechanisms are responsible for the scattering under excitation in resonance with the following complexes; exciton bound to neutral acceptor (A^0X) and a localized exciton neighboring as a neutral acceptor. It is demonstrated that in the Faraday backscattering geometry the A^0X-mediated scattering process can be considered as a double spin flip because it includes an acoustic-phonon-induced spin flip of an electron in the photocreated A^0X complex. In tilted magnetic fields an additional satellite line A^0X' appears in the Raman spectrum due to the Zeeman interaction of the electron spin with the in-plane field component. The neutral-acceptor and electron g factors are directly measured as a function of the quantum-well width. Two other lines of the A^0X-related scattering are attributed to the bound-hole interlevel transitions $\pm\frac{3}{2} \rightarrow \mp\frac{1}{2}$, which allow the determination of the interlevel splitting and an analysis of its inhomogeneous broadening induced by fluctuations in the well thickness.

I. INTRODUCTION

In Ref. 1 we reported strong spin-flip-related Raman scattering (SFRS) in p-type $GaAs/Al_xGa_{1-x}As$ (001)-oriented multiple quantum wells (MQW's). The experiment was performed in the backscattering Faraday configuration $z(\sigma^\eta,\sigma^\lambda)\bar{z}$, z being parallel to the heterostructure growth direction and $\eta = \pm$, $\lambda = \pm$ denoting the circular polarization of the exciting σ^η and scattered σ^λ light. It was shown that this scattering is related to transitions within the magnetic-field-split ground state of the neutral acceptor into the $\pm 3/2$ sublevels and involves the angular-momentum flips $+3/2 \rightarrow -3/2$ or $-3/2 \rightarrow +3/2$ of a hole bound to an acceptor. The effect exhibits resonance behavior and the scattering efficiency is significant only within a narrow frequency region between the low-energy edge of the photoluminescence spectrum and the fundamental-absorption edge of the heterostructure. The polarization of the Stokes and anti-Stokes components was found to depend on the excitation energy. Correspondingly, at least two different mechanisms were identified to contribute to the bound-hole-related SFRS. At the low-energy edge of the SFRS resonance profile, Stokes and anti-Stokes lines are observed in the $z(\sigma^\mp,\sigma^\pm)\bar{z}$ configurations, respectively (scattering process A in the notation of Ref. 1). Under excitation at the high-energy edge, both Stokes and anti-Stokes lines are observed in the $z(\sigma^\eta,\sigma^\eta)\bar{z}$ configurations with their intensities being independent on the sign of η (process B in Ref. 1). The effect has been also observed in p-type $GaAs/Al_xGa_{1-x}As$ MQW's with unintentionally introduced carbon acting as an acceptor.[2]

Symmetry considerations show that the bound-hole-related SFRS is forbidden if (i) the heterostructure has no other imperfections except a substitutional acceptor atom and (ii) electron spin-lattice relaxation or electron-nuclear hyperfine interaction is neglected.[3] This can be understood by taking into account that, under a transition $\pm 3/2 \rightarrow \mp 3/2$, the hole changes the z component of its angular momentum by $\Delta J_z = \pm 3$ whereas, for the backscattering geometry, the photon angular-momentum projection either remains unchanged or changes by $\Delta\sigma = \pm 2$. The scattering process B was attributed in Refs. 1 and 3 to a three-particle complex that consists of an electron-hole pair in a resonantly photoexcited localized exciton and an equilibrium hole bound to an acceptor in the vicinity of the localization area. As a result of the hole-hole "flip-stop" interaction[4] $(m, m_A) \rightarrow (m, -m_A)$ the acceptor-bound hole changes its spin from $m_A = \pm 3/2$ to $-m_A$ whereas the spin m of the hole in the exciton remains the same. This implies that the polarizations σ^η and σ^λ coincide. The symmetry is broken by the in-plane anisotropy of such a complex (see details in Ref. 3). While no alternative to this microscopic explanation of process B is available, the interpretation of process A is not so transparent since, in this case, the spins of all three particles should be reversed. Of course it can be described purely in terms of exchange interaction[1,3] but such an explanation includes two weak exchange couplings, one of them being the flip-stop transition $(m, m_A) \rightarrow (-m, m_A)$ and the other the inversion $(\pm 1/2, \pm 3/2) \rightarrow (\mp 1/2, \mp 3/2)$ of electron and hole spins in the exciton. The latter spin flip is allowed by the tetragonal symmetry of the $GaAs/Al_xGa_{1-x}As$ (001)

MQW structure. Alternative mechanisms for the electron spin flip were suggested in Refs. 1, 3, and 7.

In the present work we show that excitons bound to neutral acceptors contribute to SFRS process A. These complexes act as resonant intermediate states and scattering occurs due to acoustic-phonon-assisted spin flip of electrons in the exciton. As a result, the Raman shift is determined by both hole and electron g factors. This interpretation is unambiguously verified in experiments at tilted magnetic fields in which no-phonon bound-carrier SFRS becomes allowed in addition to the acoustic-phonon-assisted SFRS. Therefore the tilted-field experiments enable us to make direct measurements not only of the acceptor-bound hole but also of the electron g factor and to obtain their dependence on well width.

In addition to the strongest $\pm 3/2 \rightarrow \mp 3/2$ SFRS lines we have also observed two other lines. Their polarization properties and magnetic-field behavior indicate that they originate from the $+3/2 \rightarrow -1/2$ and $-3/2 \rightarrow +1/2$ interlevel transitions. The neutral-acceptor ground state of Γ_8 symmetry is fourfold degenerate in a bulk GaAs crystal. Because of the confinement effect of the barriers, this state splits into two close-lying levels h and l with the hole spin components $\pm 3/2$ and $\pm 1/2$, respectively.[8] In the following we refer the hole energy E to the zero-field position of the h level and introduce g factors g_h and g_l for the levels h and l such that under a magnetic field B parallel to z the energies of the four sublevels are given by

$$E_{h,\pm 3/2} = (\pm \tfrac{3}{2}) g_h \mu_0 B,$$
$$E_{l,\pm 1/2} = \Delta_C + (\pm \tfrac{1}{2}) g_l \mu_0 B, \quad (1)$$

where Δ_C is the zero-field h-l splitting and μ_0 the Bohr magneton. Note that the g factor g_A used in Ref. 1 is related to g_h by $g_A = 3g_h$. In a first approximation, the values of g_h and g_l coincide. The dependence of Δ_C on well width obtained from our interlevel Raman scattering measurements is in good agreement with that calculated and measured in Ref. 8.

II. EXPERIMENT

A. Spectral composition of the edge photoluminescence

In this work we used the same set of p-type $GaAs/Al_xGa_{1-x}As$ ($x = 0.33$) MQW samples with (46/110) Å, and (72/110) Å, (102/110) Å well and barrier widths and the same experimental techniques as described in the previous paper.[1]

As an example we show in Fig. 1 the luminescence spectrum (solid line) of the (72/110) Å MQW excited at $\hbar\omega = 1.7$ eV. All studied samples show three bands in the edge photoluminescence spectra.

(a) The band A^0X is associated with excitons bound to neutral acceptors. The point symmetry of a substitutional atom in a GaAs-based QW structure grown along the [001] axis is C_{2v}. If we neglect inversion-asymmetry-induced effects, the structure with an impurity atom at the center of a well can be assumed to have C_{4v} symmetry. Off-center impurities will have C_{2v} symmetry but their random distribution is expected to restore the C_{4v} symmetry in experimental observations. The analysis of our SFRS data obtained at normal and tilted magnetic fields (see below) shows that C_{4v} symmetry properties can be assigned only to the A^0X complexes contributing to the lower-energy part of the band. Other A^0X complexes are perturbed by interface roughness which reduces the symmetry and generally leads to a decrease in the binding energy of the complex. We believe that these distorted complexes [labeled $(A^0X)_d$] form the high-energy region of the A^0X band.

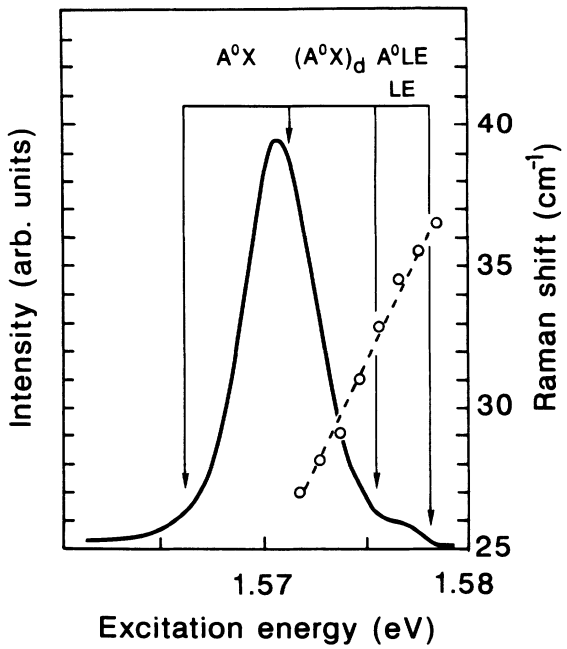

FIG. 1. Luminescence spectrum of the (72/110) Å $GaAs/Al_{0.33}Ga_{0.67}As$ sample at $T = 6$ K and $B = 0$ taken at an excitation energy of $\hbar\omega = 1.7$ eV. Labels A^0X, $(A^0X)_d$, and A^0LE/LE indicate the energy ranges in which the different exciton complexes contribute to the emission. See text (Sec. II A) for details. Open circles give the Raman shift of Δ_C vs excitation energy (see discussion in Sec. II B) at $B = 0$. The dashed line is a guide to the eye.

(b) The localized excitons (LE) band is associated with excitons localized on interface imperfections. The ratio of emission intensities for A^0X and LE bands varies from 3 [(46/100) Å sample] to 10 [(102/110) Å sample] thus reflecting the higher density of LE states in relatively narrow QW's. From the resonance profile of the SFRS efficiency we distinguish the contribution of three-particle complexes which can be considered as a localized exciton neighboring a neutral acceptor and weakly perturbed by it. For such complexes we use the notation A^0LE. It is clear that their contribution to the photoluminescence spectrum overlaps with the high-energy tail of the A^0X band.

(c) The band e-A^0, located at 1.543 eV and not shown in Fig. 1, arises from radiative recombination of free and/or localized single electrons with holes bound to neu-

tral acceptors. It is observed only under above-gap optical excitation.

B. SFRS in the Faraday configuration

Under excitation slightly above the maximum of the A^0X band, three Stokes Raman lines and three anti-Stokes lines are observed in the Faraday geometry. The scattering lines are active only in either (σ^+,σ^-) or (σ^-,σ^+) crossed polarizations, as can be seen from Fig. 2 where Raman spectra in the Stokes region are presented for two scattering configurations. The Stokes shift ΔE of the lines is plotted as a function of applied magnetic field in Fig. 3 for the two (102/110) Å (full circles) and (72/110) Å (open circles) GaAs-$Al_{0.33}Ga_{0.67}As$ samples. Up to $B = 14$ T the value of ΔE for each line varies linearly with the field. For clarity we illustrate the neutral-acceptor energy levels in the inset to Fig. 3. The strongest line, marked as $-3/2 \rightarrow +3/2$, corresponds to the transition between the magnetically split sublevels $\pm 3/2$ of a neutral acceptor. For vanishing magnetic field the Raman shift of this line tends to zero in accordance with Eq. (1), which gives for the Stokes shift $\Delta E(-3/2 \rightarrow +3/2) = 3g_h\mu_0 B$. The two other lines marked $-3/2 \rightarrow +1/2$ and $+3/2 \rightarrow -1/2$ are related to interlevel Raman scattering. With decreasing magnetic field their shifts approach the same nonzero

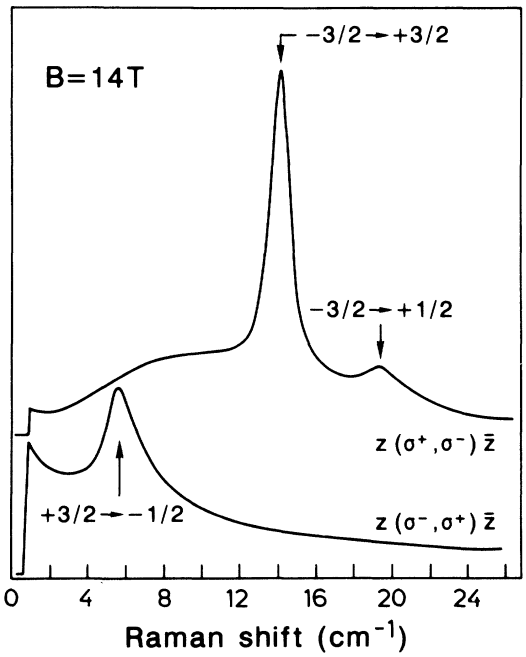

FIG. 2. Raman spectra measured in the (102/110) Å GaAs-$Al_{0.33}Ga_{0.67}As$ sample in (σ^+,σ^-) (upper spectrum) and (σ^-,σ^+) (lower) configurations in a magnetic field $B = 14$ T at $T = 4$ K. The spectra were taken under resonance excitation of A^0X complexes ($\hbar\omega_l = 1.552$ eV) in Faraday backscattering geometry. The notation $-3/2 \rightarrow +3/2$, $+3/2 \rightarrow -1/2$, and $-3/2 \rightarrow +1/2$ labels Raman lines attributed to the corresponding transitions of an acceptor-bound hole.

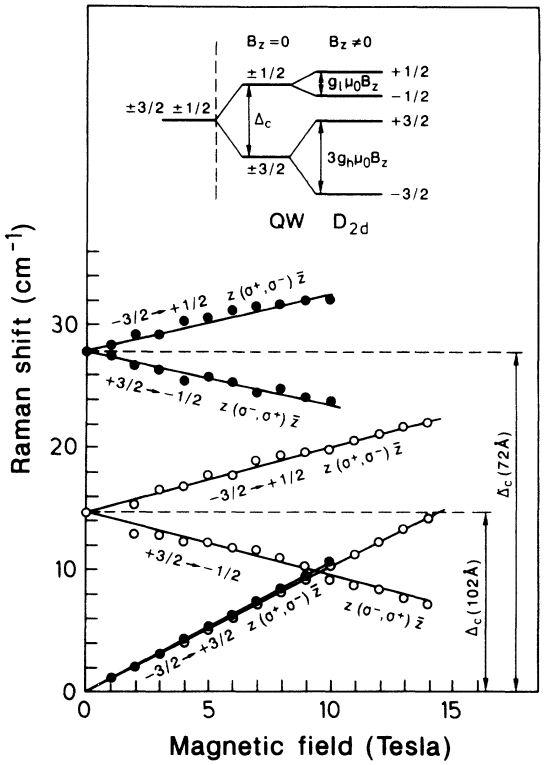

FIG. 3. Magnetic-field dependence of the Raman shifts of the $-3/2 \rightarrow +3/2$, $+3/2 \rightarrow -1/2$, and $-3/2 \rightarrow +1/2$ lines for the (102/110) Å (open circles) and (72/110) Å (full circles) GaAs-$Al_{0.33}Ga_{0.67}As$ samples. Δ_C denotes the "crystal-field" splitting of the acceptor ground state into two Kramers doublets at zero magnetic field. The inset shows the scheme of neutral acceptor energy levels at zero and nonzero z component of the magnetic field.

value since, as follows from Eq. (1), $\Delta E(m \rightarrow m') = \Delta_C + \mu_0 B(m' g_l - m g_h)$, where $m = \pm 3/2$ and $m' = \pm 1/2$. At zero field only one partially polarized line is observed with the same Raman shift Δ_C on the Stokes and anti-Stokes side of the spectrum. For the (102/110) Å sample the intensity ratio $I(\sigma^-,\sigma^-)/I(\sigma^-,\sigma^+)$ is close to 3 as expected from selection rules for the $\Gamma_8 \leftrightarrow \Gamma_6$ interband optical transitions in bulk GaAs.

Figure 1 also shows the dependence of Δ_C on excitation energy $\hbar\omega_l$ (open circles). One can see that the observed value of Δ_C increases monotonically with increasing $\hbar\omega_l$. This can be understood taking into consideration that the lower-energy excitation probes neutral acceptors with higher binding energy. Their states are less affected by barrier confinement and hence the splitting Δ_C is smaller. The Raman shift of the interlevel scattering displays a strong dependence on the well width, as demonstrated in Table I. The values of Δ_C reported here were obtained while probing the low-energy region of the A^0X band, i.e., presumably the unperturbed A^0X complexes. The half-width (full width at half maximum) of the interlevel scattering line at zero field (or its two components $-3/2 \rightarrow +1/2$, $+3/2 \rightarrow -1/2$ in a magnetic field) exceeds noticeably that of the SFRS line $-3/2 \rightarrow +3/2$ because the value of Δ_C should be much more sensitive to fluctuations in the well thickness and

TABLE I. Parameters of the crystal-field splitting of acceptor states, Δ_C, and the acceptor electron g factors g_h and g_e measured by SFRS for various MQW samples. For comparison theoretical values g_e^{theor} from Ref. 14 calculated for the different well widths are also given.

$GaAs/Al_xGa_{1-x}As$	Δ_C (meV)	$3g_h$	g_e	g_e^{theor}
(46/110) Å	7.3	2.4	≈ 0	0
(72/110) Å	3.5	2.18	−0.11	−0.18
(102/110) Å	2	2.09	−0.23	−0.25

other structure imperfections than the bound-hole g factor.

The Raman shift of the SFRS line $-3/2 \rightarrow +3/2$ is almost insensitive to the excitation energy when we probe the A^0X or $(A^0X)_d$ complexes but changes abruptly as the excitation energy reaches the resonance with A^0LE complexes. Two lines coexist in the scattering spectrum within the small interval of excitation energies where both A^0X and A^0LE complexes contribute to SFRS. Figure 4 shows SFRS spectra measured under excitation with three different incident-photon energies probing A^0X complexes ($\hbar\omega_1^\alpha$) or A^0LE complexes ($\hbar\omega_1^\gamma$) independently, as well as the mixed region ($\hbar\omega_1^\beta$). The energy difference between the lines arising due to A^0X and A^0LE complexes as intermediate states in the scattering process depends on the well width, varying at a fixed magnetic field of 10 T from 1.5 cm^{-1} [(102/110) Å (MQW)] to almost zero in the (46/110) Å MQW. In all samples, the SFRS from A^0X or $(A^0X)_d$ complexes is active only in crossed polarizations. On the other hand, the polarization properties of SFRS via A^0LE complexes depend on the well width, the ratio $I(\sigma^-,\sigma^-)/I(\sigma^-,\sigma^+)$ being equal to 10, 2.2, and 2.2 for the (46/110) Å, (72/110) Å, and (102/110) Å MQW's, respectively.

C. The scattering spectra under tilted magnetic fields

The main result of measurements at tilted magnetic fields is the splitting of the $-3/2 \rightarrow +3/2$ SFRS line into two components observed under resonant excitation of A^0X or $(A^0X)_d$ complexes. Figure 5 shows Raman spectra recorded from the (102/110) Å sample under magnetic fields of the same magnitude ($B = 10$ T) but for different angles ϕ between the field direction and the growth direction z. The excitation energy is chosen to coincide with the maximum of the A^0X band. The splitting can be interpreted as the appearance in the Raman spectrum of an additional satellite line, A^0X', at $\phi \neq 0$. Figure 6 displays the angular dependence of the Raman shift of the two components A^0X and A^0X'. We associate the component A^0X' with no-phonon SFRS similar to the well-known Raman scattering that occurs as a result of spin-flip transitions of donor-bound electrons or acceptor-bound holes in hexagonal bulk semiconductors or QW structures at oblique or transverse magnetic fields with respect to the principal axis z of the uniaxial crystal or heterostructure.[9] A diagram for such processes is shown in Fig. 7(a).

The component designated as A^0X in Figs. 5 and 6 was first observed in Ref. 1. It has now become clear that this line arises as a result of the following acoustic-phonon-assisted three-step process shown in Fig. 7(b): (i) resonant photogeneration of A^0X or $(A^0X)_d$ complexes which exhibit spin sublevels $s = \pm 1/2$ because the electron spin in an A^0X complex is uncompensated while the hole spins add up to zero; (ii) electron spin flip $+1/2 \rightarrow -1/2$ or $-1/2 \rightarrow +1/2$ of the photogenerated complexes induced by absorption or emission of an acoustic phonon with energy $\hbar\Omega_{ac}$ equal to the Zeeman splitting of an A^0X complex and determined by the electron g factor; (iii) annihilation of the A^0X complexes with the emission of photons in the circular polarization σ^λ opposite to the initial polarization σ^η.

The Raman shift of the A^0X' component is well described by a cosine function: $\Delta E(-3/2 \rightarrow +3/2; A^0X'; \phi) = \Delta_A \cos\phi$, where $\Delta_A = 3g_h\mu_0 B$. This

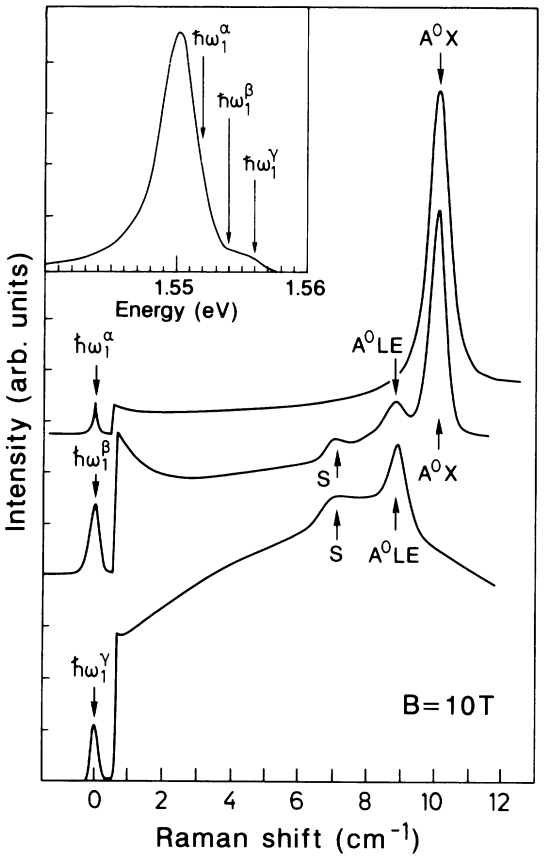

FIG. 4. Raman spectra measured in the (102/110) Å GaAs-$Al_{0.33}Ga_{0.67}As$ sample in the (σ^+,σ^-) backscattering configuration at $B = 10$ T for three different excitation energies: $\hbar\omega_1^\alpha = 1.552$ eV (resonance excitation of A^0X complexes), $\hbar\omega_1^\gamma = 1.556$ eV (resonance excitation of A^0LE complexes, $\hbar\omega_1^\beta = 1.554$ eV (the region of overlapping A^0X and A^0LE photoluminescence bands). Labels A^0X and A^0LE indicate $-3/2 \rightarrow +3/2$ spin-flip scattering related to the respective complexes. S denotes an unidentified structure. The inset shows the photoluminescence spectrum of this sample. The arrows labeled $\hbar\omega_1^\alpha$, $\hbar\omega_1^\beta$, and $\hbar\omega_1^\gamma$ mark the excitation energies at which the respective Raman spectra were taken.

indicates that the transverse g factor $g_h^{\perp}$ of a ground-state bound hole is close to zero. The Raman shift of the A^0X component, however, must be described by the function $\Delta_e + \Delta_A \cos\phi$ with a nonvanishing term Δ_e which reflects the fact that both the longitudinal and transverse components of the electron g factor are nonzero. The values of Δ_e and Δ_A are different for the (72/110) Å and (102/110) Å samples (see Table I). For the (46/110) Å sample, the splitting of the $-3/2 \rightarrow +3/2$ line at $\phi = 0$ and $B = 10$ T was not resolved and only an increase in the linewidth from 0.6 cm^{-1} for $\phi = 0$ to 1.5 cm^{-1} for $\phi = 30°$ was observed. The Raman shift of this line in the (46/110) Å sample shows a cosine dependence (with $\Delta_e \simeq 0$) as has been reported earlier (see Fig. 6 of Ref. 1).

The ratio of intensities of the A^0X and A^0X' components is angle dependent. At $\phi = 0$ only the A^0X-related Raman component at larger Raman shifts is present in the SFRS spectrum. With increasing ϕ the A^0X' component is enhanced and for $\phi = 30°$ the two intensities become comparable. A further increase in ϕ changes the intensity ratio in favor of the A^0X' component and for $\phi \geq 60°$ the A^0X component becomes negligible. While the splitting between the A^0X and A^0X' components is insensitive to the excitation energy $\hbar\omega_1$, the ratio of their intensities is a strong function of $\hbar\omega_1$. This is clearly illustrated in the spectra 3 and 3* of Fig. 5 which were

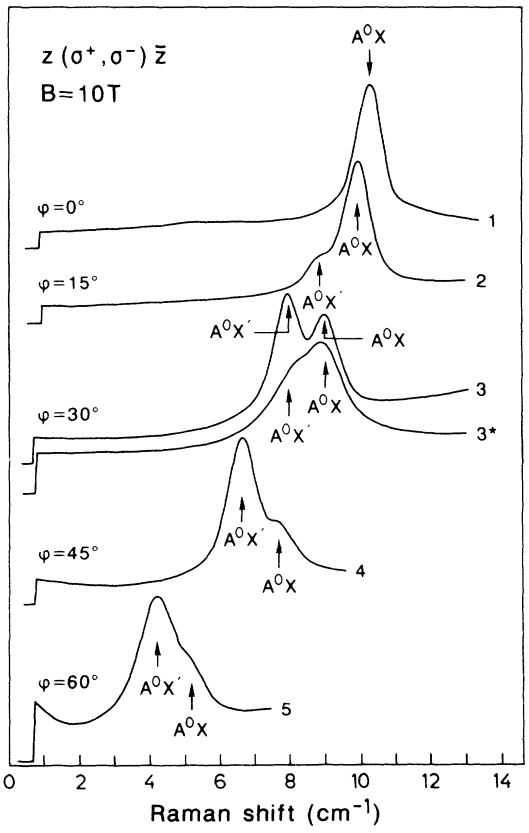

FIG. 5. Raman spectra measured in the (102/110) Å GaAs-$Al_{0.33}Ga_{0.67}As$ sample at fixed magnetic field $B = 10$ T and different angles ϕ between the magnetic field B and the MQW growth direction. In each case the excitation energy $\hbar\omega_1$ is tuned to be in resonance with A^0X complexes. The spectra 3 and 3* were taken at the same angle under resonant (3: $\hbar\omega_1 = 1.549$ eV) and off-resonant (3*: $\hbar\omega_1 = 1.55$ eV) excitation, respectively. The peaks marked as A^0X and A^0X' correspond to the $A1$-type and $A3$-type scattering processes discussed in Sec. III B.

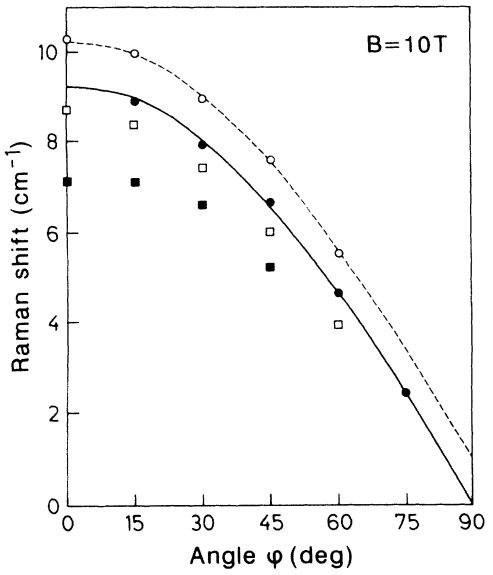

FIG. 6. Angular dependence of the Raman shift for the $-3/2 \rightarrow +3/2$ spin-flip scattering lines in the (102/110) Å sample at fixed $B = 10$ T. Open and full circles represent the A^0X and A^0X' components observed under resonant excitation of A^0X complexes, connected with $A1$- and $A3$-type processes in the notation of Sec. III B. The open and full squares indicate the position of the $\mp 3/2 \rightarrow \pm 3/2$ line and its low-energy shoulder observed under resonant excitation of A^0LE complexes. The dashed line represents $\Delta_e + \Delta_h \cos\phi$ while the solid line corresponds to the cosine function $\Delta_A \cos\phi$.

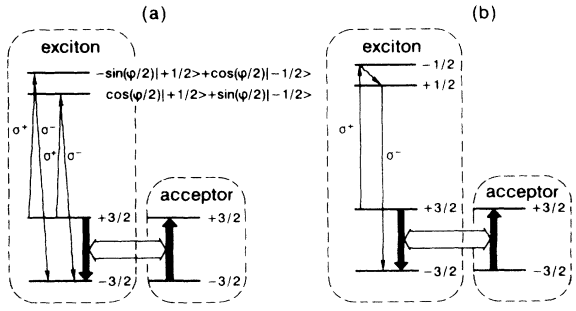

FIG. 7. Illustration of A^0X-related Raman scattering processes leading to the $-3/2 \rightarrow +3/2$ spin flip of acceptor-bound holes. (a) $A3$-type processes discussed in Sec. III B and realized only in tilted magnetic fields. (b) $A1$-type process that takes place both in the exact Faraday backscattering geometry and in tilted magnetic fields. The up (down) arrows describe the optical excitation (annihilation) of an acceptor-bound exciton. Bold arrows illustrate flip-flop of angular momenta of a hole in the exciton and an acceptor-bound hole due to hole-hole exchange interaction (double arrow). The wavy arrow represents the electron spin-lattice relaxation.

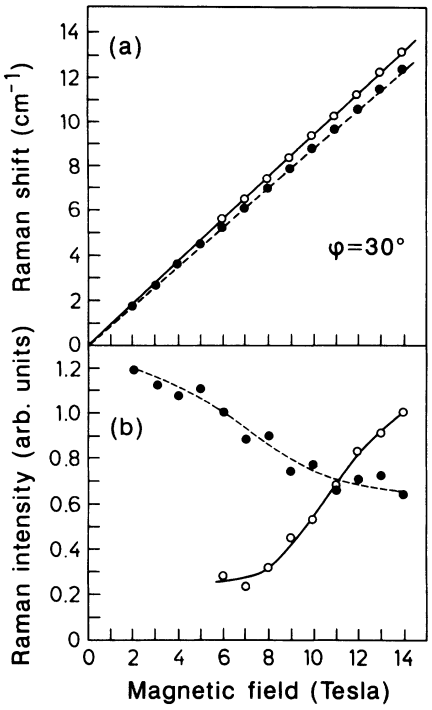

FIG. 8. (a) Raman shift and (b) intensity vs tilted magnetic field B ($\phi = 30°$) for the (72/110) Å sample under optical excitation in resonance with A^0X complexes. The open and full circles correspond to the A^0X and A^0X' components of the $-3/2 \rightarrow +3/2$ Raman line, respectively. The solid and dashed curves in (b) are guides to the eye.

recorded under the same conditions except for different excitation energies. The influence of the magnetic field on the Raman shift and intensity of the A^0X and A^0X' components is illustrated in Fig. 8 [(72/110) Å sample, $\phi = 30°$].

Under resonant excitation of the A^0LE complexes, a weak shoulder at the smaller-Raman-shift side is observed in addition to the sharp SFRS line (see features labeled S and A^0LE in the spectra taken at $\hbar\omega_1^\beta$ and $\hbar\omega_1^\gamma$ in Fig. 4). In the Raman spectra taken from the (46/110) Å sample this shoulder is absent but instead the SFRS line is asymmetric. In a tilted magnetic field this line does not exhibit any splitting. An increase in the angle φ is accompanied by a decreasing Raman shift (see Fig. 6) and an increasing relative intensity of the shoulder.

We have measured as well the angular dependence of Raman shifts for the interlevel-scattering lines. At $B =$ 10 T, the Raman shift of the $+3/2 \rightarrow -1/2$ line decreases by 1.5 cm^{-1} when the angle change from $\phi = 0$ to $\phi =$ 60° while an increase in the shift by the same value is observed for the $-3/2 \rightarrow +1/2$ line.

III. THEORY AND DISCUSSION

A. Scattering due to flip-stop hole-hole exchange interaction

We shall first describe the scattering process B that occurs under resonant excitation of A^0LE complexes. In this case a $\sigma^\pm$ photon excites an A^0LE complex $|s,j,m\rangle$ with $s + j = \pm 1$, where $m = \pm 3/2$ is the initial spin of an acceptor-bound hole and $s = \pm 1/2$, $j = \pm 3/2$ are the spin indices of an electron and a hole in the photoexcited localized exciton. At the next stage the hole in the exciton induces a flip $m \rightarrow -m$ of the bound hole as a result of a flip-stop-type hole-hole exchange interaction described as[3]

$$V_{\rm exch}^{(1)} = \left(\Delta_{1-}\sigma_+^A + \Delta_{1+}\sigma_-^A\right)\sigma_z^{\rm LE}, \tag{2}$$

where $\Delta_{1-} = \Delta_{1+}^*$ and $\sigma_\pm = (\sigma_x \pm i\sigma_y)/2$. Here we use the Pauli matrices $\sigma_\alpha^{\rm LE}$, σ_α^A operating on the exciton or acceptor bound-hole states $\pm 3/2$ in the basis $2^{-1/2}(X + iY)\uparrow$, $2^{-1/2}(X - iY)\downarrow$. At the final stage the localized exciton annihilates, emitting a photon of the same polarization, but the neighboring bound hole has now the inverted spin $-m$ and the secondary photon energy $\hbar\omega_2$ differs from the initial energy $\hbar\omega_1$ by $\mp\Delta_A$, where $\Delta_A = 3g_h\mu_0B_z$ with the plus and minus signs corresponding to Stokes and anti-Stokes scattering.

We express the intensity dJ of the σ^λ-polarized light scattered backwards by a MQW structure from an area S into a solid angle $d\Omega_2^0$ outside the sample within the frequency interval $d\omega_2$ in the following form:

$$dJ = J(\sigma^\lambda, \omega_2) S d\omega_2 d\Omega_2^0. \tag{3}$$

Considering the exchange interaction as a weak perturbation we can write for the spectral intensity

$$J(\sigma^\lambda,\omega_2) = \frac{(1-R)^2}{\varepsilon(\omega_2)}\frac{1-e^{-(K_1+K_2)L}}{(K_1+K_2)d} I_1^0 \frac{1}{c^4} \times \sum_m f_m \int d\bar{\omega} g_{sj}^{\rm LE}(\bar{\omega}) \overline{|R_{sj,m}(\vec{e}_2,\vec{e}_1)|^2} \times \delta(\omega_1 - \omega_2 + 2mg_h\mu_0B_z). \tag{4}$$

Here I_1^0 is the initial light intensity, $\vec{e}_i$ the unit vector for circularly polarized light ($i = 1$ represents the incident frequency, $i = 2$ the scattered one), ε is the real part of the dielectric constant, K_i the absorption coefficient at the frequency ω_i (i = 1,2), R the reflection coefficient on the external boundary plane (the difference between R_1 and R_2 being ignored), L the length, and d the period of the MQW structure. Other notations are as follows: $\hbar\bar{\omega}$ is the localized exciton energy, $\hbar^{-1}g_{sj}^{\rm LE}(m)$ the density of energy states for localized excitons, and f_m the occupation number of the neutral-acceptor sublevel $m = \pm 3/2$. In the equilibrium one has

$$f_m = \frac{e^{-x_m}}{e^x + e^{-x}}, \quad x_m = m\frac{g_h\mu_0B_z}{k_BT}, \quad x = |x_m|, \tag{5}$$

where k_B is the Boltzmann constant. The total matrix element for a resonant scattering process is given by

$$R_{sj,m}(\vec{e}_2,\vec{e}_1) = \frac{M_{sj}^*(\vec{e}_1)\Delta_{1l}M_{sj}(\vec{e}_1)}{\hbar^2(\bar{\omega} - \omega_2 - i\gamma)(\bar{\omega} - \omega_1 - i\gamma)}\delta_{\lambda\eta}, \tag{6}$$

where $l = 1$ if the initial bound-hole spin m is $-3/2$ and $l = -1$ if $m = 3/2$, γ is the damping constant of a localized exciton connected with its lifetime τ by $\gamma =$

$(2\tau)^{-1}$, and $M_{sj}(\vec{e})$ is the matrix element of the localized-exciton photoexcitation, which can be written as

$$M_{sj}(\vec{e}) = \frac{e}{m_0}(\vec{p}_{s,-j}, \vec{e}) \int \Phi(\vec{R}, \vec{R}) d\vec{R}, \tag{7}$$

$\Phi(\vec{r}_e, \vec{r}_h)$ being the exciton envelope function and $\vec{p}_{s,-j}$ the interband matrix element of the momentum operator (m_0 is the free electron mass). The bar over $|R_{sj,m}|^2$ in Eq. (4) indicates that the value of $|\Delta_{1l}|^2$ is averaged over a spatial distribution of acceptors. Note that for simplicity we have neglected in Eq. (4) both homogeneous and inhomogeneous broadening of the SFRS line.

Neglecting also the variation of $g_{sj}^{\mathrm{LE}}(\bar{\omega})$ within an interval of the width γ we can integrate in Eq. (4) over $\bar{\omega}$ as shown below:

$$\int \frac{g^{\mathrm{LE}}(\bar{\omega}) d\bar{\omega}}{|(\bar{\omega} - \omega_2 - i\gamma)(\bar{\omega} - \omega_1 - i\gamma)|^2} = \frac{2\pi\hbar^2\tau}{\Delta_A^2}[g(\omega_1) + g(\omega_2)]. \tag{8}$$

If we introduce the partial contribution K^{LE} to the absorption coefficient due to photogeneration of localized excitons then the SFRS efficiency can be written for the Stokes or anti-Stokes component in the following final form:

$$J^B_{\mathrm{SFRS},\lambda} \equiv \int J(\sigma^\lambda, \omega_2) d\omega_2 = I_1^0 \frac{(1-R)^2}{2\pi\sqrt{\varepsilon}} \left[1 - e^{-(K_1+K_2)L}\right] \delta_{\lambda\eta} \times \frac{K_1^{\mathrm{LE}} + K_2^{\mathrm{LE}}}{K_1 + K_2} \frac{e^2}{\hbar c} \frac{\overline{|\Delta_{1l}|^2}}{\Delta_A^2} \frac{p_{cv}^2}{m_0^2 c^2} f_m \omega\tau, \tag{9}$$

where $p_{cv} = i\langle S|p_x|X\rangle$ and ω can be ω_1 as well as ω_2. We can also present $J^B_{\mathrm{SFRS},\lambda}$ in the equivalent form

$$J^B_{\mathrm{SFRS},\lambda} = \frac{1 - e^{-(K_1+K_2)L}}{(K_1+K_2)d} 2 \frac{\overline{|\Delta_{1l}^2|}}{\Delta_A^2} J_{R,\lambda}, \tag{10}$$

where

$$J_{R,\lambda} = 1/2\,[J_{R,\lambda}(\omega_1) + J_{R,\lambda}(\omega_2)]$$

and $J_{R,\lambda}(\omega)$ is the contribution of localized excitons in one particular QW to the Rayleigh (or elastic) resonant scattering, which physically is quite similar to the resonant fluorescence of atoms.

Let us now consider a bound exciton localized in the (x,y) plane within an area δS and let us assume that Δ_1^2 is a characteristic value of $|\Delta_{1\pm}|^2$ for A^0LE complexes. Then one can estimate $\overline{|\Delta_{1l}|^2}$ in Eqs. (9) and (10) as $N_A \delta S \Delta_1^2$, N_A being the two-dimensional (2D) acceptor density in a QW. Hence the corresponding scattering efficiency is proportional to N_A.

While deriving Eqs. (4), (6), and (9) we assumed weak hole-hole and electron-hole exchange interactions compared with the Zeeman splitting of hole states. The general case of arbitrary ratios between the flip-flop-like hole-hole exchange constant, the electron-hole exchange constant, and the Zeeman energies is analyzed in Ref. 3.

B. Resonant scattering involving A^0X and $(A^0X)_d$ complexes

The effective Hamiltonian describing the lower levels of an A^0X complex confined in the QW can be written in the form (see, e.g., Ref. 10)

$$H = \Delta_{hh}\vec{J}_1 \cdot \vec{J}_2 + \Delta_{eh}(\vec{J}_1 + \vec{J}_2) \cdot \vec{s} - \frac{\Delta_C}{2}(J_{1z}^2 + J_{2z}^2) + \bar{g}\mu_0 \vec{B} \cdot (\vec{J}_1 + \vec{J}_2) + g_e^{\parallel}\mu_0 B_z s_z + g_e^{\perp}\mu_0 \vec{B}_\perp s_z. \tag{11}$$

The exchange interaction between the three particles, an electron and two holes, is represented by the first two terms. In bulk GaAs, the constants Δ_{hh} and Δ_{eh} are both negative. This follows from the fact that the ground state of an A^0X acceptor is characterized by the total angular momentum $J = 5/2$.[11] The photoluminescence excitation spectra measured in $GaAs/Al_xGa_{1-x}As$ MQW's (Ref. 10) show that the negative sign of Δ_{hh}, Δ_{eh} is also retained in QW structures. The third term in Eq. (11) accounts for confinement-induced splitting of the Γ_8 acceptor states into the levels h ($\pm 3/2$) and l ($\pm 1/2$) (the crystal-field splitting, see the inset in Fig. 2). The Zeeman effect is described by the last three terms in Eq. (11), where we take into consideration the possible anisotropy of the electron g factor and neglect the anisotropic Zeeman term for the hole proportional to $\Sigma_\alpha B_\alpha J_\alpha^3$ ($\alpha = x,y,z$) in which case $g_h = g_l = \bar{g}$. We assume for simplicity that the hole g factor in the A^0X complex is the same as that of a simple acceptor state. For the $(A^0X)_d$ complex the effective Hamiltonian contains additional symmetry-reducing terms proportional to the matrices $\{J_{i\alpha}J_{i\beta}\}$ (i=1,2; $\alpha,\beta = x,y,z$) where $\{AB\}$ means $(AB+BA)/2$.

The spin properties of the lower levels in the A^0X complex essentially depend on the relationship between the constants Δ_C, Δ_{hh}, and Δ_{eh}. Holtz *et al.*[10] used quantum wells selectively doped with Be in the central 20% of the QW. In this case, for a 100 Å wide QW, the exchange splitting evidently dominates over the crystal-field splitting $\Delta_C \approx 0.65$ meV. In our Be-doped samples, only two monolayers of GaAs next to the $GaAs/Al_xGa_{1-x}As$ interfaces were left undoped.[1] The remarkably large values of Δ_C (see Fig. 3 and Table I) provide evidence that A^0X complexes with off-center acceptors are mainly responsible for Raman scattering in our samples.

For large enough h-l splitting of neutral-acceptor states, the zero-field ground level of A^0X complexes in a QW is doubly degenerate and characterized by the uncompensated spin $s = \pm 1/2$. The spin structure of the Kramers-conjugate states is as follows:

$$|A^0X, s\rangle = C_1|\pm\tfrac{3}{2}, \pm\tfrac{3}{2}; s\rangle + C_2|\pm\tfrac{1}{2} \pm \tfrac{1}{2}; s\rangle + C_3|3s, -s; -s\rangle. \tag{12}$$

Here we denote by $|m_1, m_2; s\rangle$ the state with hole angular

momenta m_1, m_2 and electron spin s. In the Γ_8 basis used in Ref. 3 the coefficients C_l (l=1,2,3) are s independent. In first approximation they are given by

$$C_1 = 1, \quad C_2 = \frac{3}{4}\frac{\Delta_{hh}}{\Delta_C}, \quad C_3 = -\frac{\sqrt{3}}{2}\frac{\Delta_{eh}}{\Delta_C}. \tag{13}$$

A considerable contribution to the three-particle state of Eq. (12) from the $\pm 1/2$ hole state enables one to observe the intensive interlevel Raman scattering. Selection rules for this scattering are easily deduced from Eq. (12). Since the selection rules allow generation of $|\mp 1/2, \pm 3/2\rangle$ excitons by $\sigma^{\pm}$ photons, the σ^{η} circularly polarized light can convert $-\eta 3/2$ neutral acceptors into $|A^0X, -\eta 1/2\rangle$ complexes with the generation rate being proportional to f_m, where $m = -\eta 3/2$ [see Eq. (5)]. Due to the admixture of $\pm 1/2$ holes, i.e., as far as the coefficient C_2 in Eq. (12) is nonzero, the electron $s = -\eta 1/2$ in the complex can recombine radiatively with the hole $-\eta 1/2$ emitting a $\sigma^{-\eta}$ photon and leaving the neutral acceptor in the final state $\eta 1/2$. Thus the selection rules for this particular kind of resonant Raman scattering can be presented in the form

$$\sigma^{\eta} + (h, -\eta\tfrac{3}{2}) \rightarrow \sigma^{-\eta} + (l, \eta\tfrac{1}{2}).$$

One can see that the total z component of the angular momentum is conserved in this process.

The efficiency of spin flip Raman scattering via A^0X complexes can be derived by applying the theory of resonant secondary emission. The final result may be written as

$$J^A_{\mathrm{SFRS},\lambda} = \frac{1 - e^{-(K_1+K_2)L}}{(K_1+K_2)d} Q J_{R,\eta}\delta_{\lambda,-\eta}. \tag{14}$$

Here K_i is the light absorption coefficient at the frequency ω_i in the polarization σ^{η} (i = 1) and $\sigma^{-\eta}$ (i = 2), and $J_{R,\lambda}$ is the contribution of A^0X complexes to Rayleigh backscattering. We have considered three different mechanisms leading to the spin reversal: ($A1$) the spin-flip of photogenerated A^0X complexes due to absorption or emission of acoustic phonons, ($A2$) the spin-flip of A^0X complexes due to the hyperfine coupling between the electronic and nuclear spins, and ($A3$) the Larmor precession of the electronic spin in the A^0X complexes in tilted magnetic fields ($\phi \neq 0$). The dimensionless factor Q in Eq. (14) and the Stokes SFRS shift $\Delta E(-3/2 \rightarrow +3/2)$ are given, respectively, by

$$Q_{A1}(\vec{B} \parallel z) = \frac{\tau}{\tau_s^{\pm}}, \ \Delta E = (3g_h - g_e^{\parallel})\mu_0 B_z, \tag{15a}$$

$$Q_{A2}(\vec{B} \parallel z) = \frac{1}{(\hbar\Omega_e^{\parallel})^2}\int \frac{d\vec{r}}{v_0}[W^e(\vec{r})]^2 \times \sum_{\nu} x_\nu^2 b_\nu I_\nu(I_\nu+1), \ \Delta E \approx 3g_h\mu_0 B_z, \tag{15b}$$

$$Q_{A3}(\phi) = \frac{1}{2}\frac{\sin^2\tilde{\phi}}{1 - \frac{1}{2}\sin^2\tilde{\phi}}, \ \Delta E = 3g_h\mu_0 B_z. \tag{15c}$$

Here τ is the lifetime of the resonant A^0X complex, $\tau_s^{\pm}$ the spin-relaxation time describing the electron spin flip induced by absorption (+) or emission (−) of an acoustic phonon, $\hbar\Omega^{\parallel} = g_e^{\parallel}\mu_0 B_z$, $W^e(\vec{r})$ the electron density in the A^0X complex, v_0 the unit cell volume, the index ν denotes the nuclear species, the factor b_ν is given by

$$b_\nu = \frac{16\pi}{3I_\nu}\mu_0\mu_\nu\eta_\nu,$$

I_ν and μ_ν are the angular momentum and the magnetic momentum of a nucleus ν, $\eta_\nu = |u(\vec{r}_\nu)|^2$, $u(\vec{r}_\nu)$ is the value of the electron Bloch function at the position of that nucleus, and x_ν is the average value of nuclei ν per unit cell. The angle $\tilde{\phi}$ is defined as $\arctan(g_e^{\perp}B_{\perp}/g_e^{\parallel}B_z)$ and $\tilde{\phi}$ differs from $\phi = \arctan(B_{\perp}/B_{\parallel})$ if the electron g factor is anisotropic. For the sake of brevity we presented the expressions for the factor Q derived assuming $|\Omega^{\parallel}|\tau \gg 1$ and $\tau_s^{\pm} \gg \tau$.

In our experiments the efficiency of SFRS due to the $A3$ mechanism equals that for the exact Faraday backscattering geometry at $\phi = 30°$. The value of Q_{A2} can be evaluated using the parameters taken from Ref. 12. The comparison between Q_{A2} and $Q_{A3}(\phi = 30°)$ shows that the hyperfine interaction does not play an important role in the scattering via A^0X complexes. Comparing Eqs. (15a) and (15c) we estimate the ratio $\tau/\tau_s^{\pm}$ as 0.1. The most probable mechanism of spin-lattice relaxation in A^0X complexes is likely to be the admixture of the $|3s, -s; -s\rangle$ state to $|A^0X, s\rangle$ [see Eq. (12)]. In this case the matrix element of the acoustic-phonon-assisted spin flip (say, $1/2 \rightarrow -1/2$) is proportional to

$$C_1C_3(\langle\tfrac{3}{2}, -\tfrac{3}{2}; -\tfrac{1}{2}|\hat{V}|\tfrac{3}{2}, -\tfrac{1}{2}; -\tfrac{1}{2}\rangle + \langle -\tfrac{3}{2}, \tfrac{1}{2}; \tfrac{1}{2}|\hat{V}|\tfrac{3}{2}, -\tfrac{3}{2}; \tfrac{1}{2}\rangle) = 2C_1C_3\langle\tfrac{3}{2}, -\tfrac{3}{2}; -\tfrac{1}{2}|\hat{V}|\tfrac{3}{2}, -\tfrac{1}{2}; -\tfrac{1}{2}\rangle,$$

where $\hat{V}$ is the perturbation operator describing the interaction of Γ_8 holes with acoustic phonons. In this connection it is worth mentioning that the presence of the last term in the right-hand side of Eq. (12) also leads to a renormalization in the g factor of an A^0X complex as compared to the electron g factor: $g^{\perp}(A^0X) = g_e^{\perp} + 2\sqrt{3}\,C_3\bar{g} = g_e^{\perp} - 3\,(\Delta_{eh}/\Delta_C)\,\bar{g}$ while $g^{\parallel}(A^0X) - g_e^{\parallel} \propto C_3^2$.

Experimental values of the electron g factor found from the analysis of the SFRS doublet line under tilted magnetic field are given in Table I. These values represent the longitudinal component $g_e^{\parallel}$ and are close to those for $g_e^{\perp}$ obtained by Snelling *et al.*[13] from Hanle effect measurements under polarized optical pumping of $GaAs/Al_xGa_{1-x}As$ QW's. For comparison, theoretical values g_e^{theor} calculated in Ref. 14 are also given. Note that these calculations were made with a two-band $k \cdot p$ model and a correction Δg of −1.3 was added in order to include effects of higher conduction bands.[14,15] Within the accuracy of our experiment we cannot confirm the electron g factor anisotropy predicted by Ivchenko and Kiselev[14] and observed by Kalevich and Korenev[16] in op-

tical orientation experiments at oblique magnetic fields. Theory predicts a large anisotropy of g_e for narrow QW's. However, we were only able to measure the angular dependence of g_e in the wider (102/110) Å quantum well (see Fig. 6). We were not able to measure the angular dependence of g_e in the (71/110) Å QW, because the two SFRS lines were only observed in a very narrow range of angles ϕ. But we did not see the splitting of the SFRS lines for the (46/110) Å QW, where the theory predicts $g_e^{\parallel} \sim 0$ and $g_e^{\perp} \simeq +0.14$.

As a possible explanation we should keep in mind the fact that we do not measure the g_e's of free electrons, but those of electrons in bound excitons, which may be modified as discussed above. We expect that the SFRS technique may yield both $g_e^{\parallel}$ and $g_e^{\perp}$ values in center-δ-doped QW's.

Raman scattering due to the interlevel transitions $\pm 3/2 \rightarrow \mp 1/2$ arises in second order perturbation theory if, as discussed above, the admixture of $\pm 1/2$ hole states in the A^0X-complex wave function is taken into account. In the tilted magnetic field, the corresponding Stokes shift is given by

$$\Delta E\,(\pm 3/2 \rightarrow \mp 1/2) = \Delta_C \mp \bar{g}\mu_0 B \left(\sqrt{\cos^2\phi + 4\sin^2\phi} + \tfrac{3}{2}\cos\phi \right), \quad (16)$$

where, as above, the hole angular momentum components are referred to the growth direction z and we assume that ϕ lies between 0 and 90°. If $90° < \phi < 180°$, then the sign of the square root in Eq. (16) should be reversed. It should be noted that Eq. (16) is valid if the Zeeman energy $\bar{g}\mu_0 B$ is small compared to the zero-field crystal splitting Δ_C. In this case the Zeeman splitting of the levels $h(\pm 3/2)$ and $l(\pm 1/2)$ can be considered independently, the former being characterized by the longitudinal g factor $3\bar{g}$ and zero transverse g factor, while the latter is characterized by $g_l^{\parallel} = \bar{g}$ and $g_l^{\perp} = 2\bar{g}$. In the experiment the Raman shift for the $+3/2 \rightarrow -1/2$ line decreases by 1.5 cm^{-1} and that for the $-3/2 \rightarrow +1/2$ line increases by the same value with a variation of ϕ from 0 to 60° (for $B = 10$ T). This is close to the change of ∓ 1.2 cm^{-1} in the interlevel Raman shift predicted by Eq. (16) for the value $\bar{g} = 0.7$ found from the SFRS shift.

IV. CONCLUSIONS

Strong spin-flip Raman scattering has been observed in p-doped MQW's under excitation in resonance with A^0X complexes as well as under resonant excitation of acceptor-neighboring localized excitons (A^0LE complexes). For A^0X-mediated scattering, three polarized Raman lines observed in a magnetic field are interpreted as angular-momentum flip of an acceptor-bound hole via exchange interaction with a photocreated exciton. The Raman shift of the most intense line tends to zero for vanishing magnetic field. This line is due to acceptor-bound hole flips $\pm 3/2 \rightarrow \mp 3/2$, which change the z component of the hole angular momentum by ± 3 and the incident photon spin by ± 2. We demonstrated, both theoretically and experimentally, that in exact Faraday backscattering geometry, such a process includes relaxation of the electron spin in the A^0X or $(A^0X)_d$ complex. The latter occurs as a result of the emission or absorption of an acoustic phonon with an energy equal to the Zeeman splitting of electron spin states. Therefore the process as a whole can be considered as a double spin flip with the Raman shift dependent on the Zeeman energies of both an acceptor-bound hole and an electron in the A^0X complex. In tilted magnetic fields the electron can change its spin due to Zeeman interaction with the in-plane field component. This results in the appearance of an additional Raman line with a shift being governed only by the neutral-acceptor Zeeman splitting and its intensity depending strongly on the angle between the magnetic field and the growth direction. Thus, by using the Raman technique, we were able to measure directly both the neutral-acceptor and electron g factors as a function of the QW width.

With decreasing magnetic field the two other A^0X-related Raman lines merge and approach a zero-field position shifted by a finite value with respect to the incident photon energy. These lines are attributed to the interlevel transitions $\pm 3/2 \rightarrow \mp 1/2$ of bound holes with an angular momentum change by ± 2. As a result we could trace the behavior of the h-l splitting Δ_C between the $\pm 3/2$ and $\pm 1/2$ neutral acceptor levels in QW's with QW width variation. The interlevel scattering can be described taking into account the hole-hole exchange interaction in the A^0X complex and an admixture of $\pm 1/2$ holes in the complex ground state.

For A^0LE-related scattering, the Raman line due to the acceptor-bound hole spin flip $\pm 3/2 \rightarrow \mp 3/2$ is explained in terms of acceptor-neighboring localized excitons and anisotropic hole-hole exchange interaction. The anisotropic "flip-stop"-type interaction leads to an inversion of the bound-hole angular momentum leaving the photocreated exciton in the same state. This explanation is also confirmed by the fact that the Raman shift for the A^0LE-related scattering is smaller than that for the A^0X-related double-spin-flip Raman scattering observed in the Faraday configuration.

ACKNOWLEDGMENTS

We are grateful to Professor B. P. Zakharchenya for useful discussions Dr. A. A. Sirenko and Dr. A. Fainstein for a critical reading of the manuscript, and Professor A. Scharmann for encouragement and support. We also would like to thank A. Fischer and H. P. Schönherr for the growth of the samples, and H. Hirt, M. Siemers, and P. Wurster for excellent technical assistance. One of us (V.F.S.) acknowledges financial support from the Max-Planck-Gesellschaft. The work of two of us (V.F.S. and E.L.I.) was supported, in part, by a Soros Foundation Grant awarded by the American Physical Society. V.F.S., E.L.I., and D.N.M. acknowledge financial support from the Volkswagen Foundation and the Russian Fund of Fundamental Investigations.

* On leave from A.F. Ioffe Physico-Technical Institute, Russian Academy of Science, 194021 St. Petersburg, Russia.

[1] V.F. Sapega, M. Cardona, K. Ploog, E.L. Ivchenko, and D.N. Mirlin, Phys. Rev. B **45**, 4320 (1992).

[2] D.N. Mirlin and A.A. Sirenko, Fiz. Tverd. Tela Leningrad **34**, 205 (1992) [Sov. Phys. Solid State **34**, 108 (1992)].

[3] E.L. Ivchenko, Fiz. Tverd. Tela Leningrad **34**, 476 (1992) [Sov. Phys. Solid State **34**, 254 (1992)].

[4] This interaction is similar to the contribution of $J'_{xz}S_{ix}S_{jz} + J'_{yz}S_{iy}S_{jz}$ to the spin-spin Hamiltonian of the magnetic ions that induces transitions with $\Delta m_i = \pm 1$, $\Delta m_j = 0$, where i and j are numbers of two ions and m_i, m_j are the eigenvalues of the spin operators S_{iz}, S_{jz} (Refs. 5, 6).

[5] A. Abragam and M.H.L. Price, Proc. R. Soc. London Ser. A **205**, 135 (1951).

[6] A. Abragram and B. Bleaney, *Electron Paramagnetic Resonance of Transitions Ions* (Clarendon Press, Oxford, 1970).

[7] V.F. Sapega, T. Ruf, M. Cardona, K. Ploog, E.L. Ivchenko, and D.N. Mirlin, in *Proceedings of the XIII International Conference on Raman Spectroscopy*, edited by W. Kiefer, M. Cardona, G. Schaack, F.W. Schneider, and H.W. Schroetter (Wiley, New York, 1992), p. 856.

[8] D. Gammon, R. Merlin, W.T. Masselink, and H. Morkoç, Phys. Rev. B **33**, 2919 (1986).

[9] G.D. Thomas and J.J. Hopfield, Phys. Rev. **175**, 1021 (1968).

[10] P.O. Holtz, Q.X. Zhao, B. Monemar, M. Sundaram, J.L. Merz, and A.C. Gossard, Phys. Rev. B **47**, 15 675 (1993).

[11] A.M. White, P.J. Dean, and B. Day, J. Phys. C **7**, 1400 (1974).

[12] D. Paqet, G. Lampel, B. Sapoval, and V.I. Safarov, Phys. Rev. B **15**, 5780 (1977).

[13] M.J. Snelling, G.P. Flinn, A.S. Plaut, R.T. Harley, A.C. Tropper, R. Eccleston, and C.C. Phillips, Phys. Rev. B **44**, 11 345 (1991).

[14] E.L. Ivchenko and A.A. Kiselev, Fiz. Tekh. Poluprovodn. **26**, 1471 (1992) [Sov. Phys. Semicond. **26**, 827 (1992)].

[15] M. Cardona, N.E. Christensen, and G. Fasol, Phys. Rev. B **38**, 1806 (1988).

[16] V.K. Kalevich and V.L. Korenev, Pis'ma Zh. Eksp. Teor. Fiz. **56**, 257 (1992) [JETP Lett. **56**, 253 (1992)].